Journal of Organometallic Chemistry 904 (2019) 121014

Contents lists available at ScienceDirect

Journal of Organometallic Chemistry

journal homepage: www.elsevier.com/locate/jorganchem

# Computational study of regiodivergent pathways in the copper-catalyzed borocyanation of 1,3-dienes: Mechanism and origin of regioselectivity

Xianming Guo, Ting Wang, Yinjian Zheng, Luoyi Zhou, Juan Li*

*Department of Chemistry, Jinan University, Huangpu Road West 601, Guangzhou, Guangdong, 510632, PR China*

ARTICLE INFO

*Article history:*
Received 9 August 2019
Received in revised form
1 November 2019
Accepted 1 November 2019
Available online 4 November 2019

*Keywords:*
Density functional theory
Regioselectivity
Mechanism
Copper
1,3-Dienes
Borocyanation

ABSTRACT

Regioselective control in the Cu-catalyzed borylcyanation of nonsymmetrically substituted 1,3-dienes remains challenging. In this study, we used density functional theory calculations to elucidate the origins of ligand- and substrate-controlled regioselectivity. The mechanism rationalizes why ligand $PCy_3$ favors 1,2-borocupration while ligand XantPhos favors 4,3-borocupration for 2-substituted 1,3-dienes, and why 1-substituted, 1,2-disubstituted, and 1,3-disubstituted 1,3-dienes afford 4,3-borocupration, irrespective of the presence of bidentate or monodentate ligands. Based on established experiments and stimulated by other relevant reactions, we attempted to enrich ligands and substrates computationally. The different regioselectivities for different substrates and ligands were attributed to different electronic and steric factors.



## 1. Introduction

In the last few decades, transition-metal-catalyzed multifunctionalization reactions of C—C multiple bonds have proven to be important because they allow molecular complexity to be rapidly generated from simple precursors [1]. With increasing interest in sustainable catalysis, the use of relatively inexpensive copper catalysts, which can act as Lewis acids, π-acids, single-electron mediators, and two-electron mediators, has attracted considerable attention [2]. In recent years, Cu-catalyzed borylative transformations of nonpolar C—C unsaturated compounds, such as alkenes [3], 1,3-dienes [4], allenes [5], alkynes [6], 1,3-enynes [7], and 1,3-diynes [8], have been recognized as important approaches to accessing organoboron compounds. These processes generally form an allyl organocopper intermediate that can be then captured by various electrophiles for further chemical manipulation [9].

The cyano group is a core chemical structure found in a broad range of biologically active agents and functional materials [10]. Owing to their important biological properties and unique structural characteristics, considerable research effort has been directed toward the development of new methods for the synthesis of cyano-containing compounds. *N*-Cyano-*N*-phenyl-*p*-methylbenzenesulfonamide (NCTS) [11], which is an electrophilic cyanation reagent with low reactivity but low toxicity, has emerged as a promising reagent for nitrile synthesis. Studies on Cu-catalyzed borylcyanation using NCTS to introduce a cyano group onto styrene and allene have been reported [12]. More recently, the Procter [13] and Meng groups [14] reported Cu-catalyzed three-component coupling reactions of 1,3-dienes and diboranes using NCTS. The challenge for Cu-catalyzed borylcyanation of non-symmetrically substituted 1,3-dienes is the control of regioselectivity.

The pioneering work of Procter developed ligand-controlled catalytic methods to bias the desired regioselectivity [13]. Using different ligands (such as XantPhos and tricyclohexyl phosphine) on the copper catalyst allowed either 4,1- or 1,4-borocupration of 2-substituted 1,3-dienes, resulting in either 4,3- or 1,2-borocyanation products (Scheme 1a). However, using different ligands with 1-substituted 1,3-dienes resulted in the formation of only 4,3-borocyanation products (Scheme 1b) [14].

The number of potential reaction pathways and complexity of these processes makes detailed elucidation of the reaction mechanism challenging. Although the ligand and substrate are widely accepted to affect the reaction pathway, the details and origins of

* Corresponding author.
*E-mail address:* tchjli@jnu.edu.cn (J. Li).

https://doi.org/10.1016/j.jorganchem.2019.121014
0022-328X/

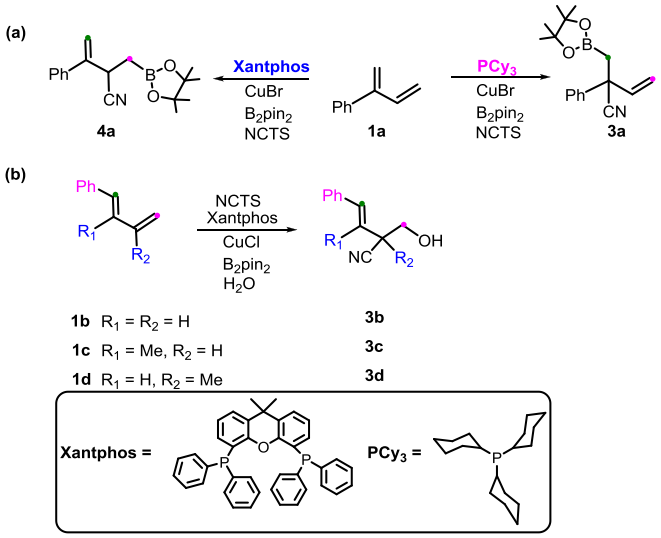


**Scheme 1.** Cu-catalyzed borylation reaction of 1,3-dienes.

these effects remain unclear. In the present work, models with different ligands and substrates were compared to study how ligands and substrates affected the reaction pathway. We believe that a deeper understanding of the mechanism will facilitate the future design of related transformations.

## 2. Computational details

All stationary points were optimized without any constraints in the solvent phase at the B3LYP level of theory [15]. Solvation effects were treated using the solvation model based on density (SMD) [16] with terahydrofuran as solvent. All calculations were performed with the Gaussian09 quantum chemical program [17]. Frequency calculations were also performed at the same level of theory to identify all stationary points as minima (zero imaginary frequencies) or transition states (one imaginary frequency), and the free energies at 298.15 K. Intrinsic reaction coordinate (IRC) calculations were performed to verify the transition state structures [18]. The Cu atom in this analysis was described using the LANL2DZ basis set, including a double-valence basis set with the Hay and Wadt effective core potential [19]. Polarization functions were added for Cu ($\zeta_f = 3.525$) [20]. The 6-31G* [21] basis set was used for other atoms. This basis set combination will be referred to as BS1. To further refine the energies obtained from the B3LYP/BS1 calculations, we carried out single-point energy calculations for all of the structures with a larger basis set (BS2) with the M06 [22] DFT method. BS2 utilizes def2-TZVP [23] for Cu and 6−311++G** for other atoms. Empirical D3 dispersion corrections for the M06 functional were included [24]. Frontier molecular orbitals and reduced density gradient (RDG) isosurface maps were generated using Multiwfn 3.6 program package [25].

## 3. Results and discussion

We first investigated the possible mechanisms of the Cu-catalyzed borylation reaction of 2-substituted 1,3-dienes using $PCy_3$ and XantPhos ligands to elucidate the overall catalytic cycle and identify the regioselectivity-determining transition states [26]. The reactions with other phosphine ligands and 1-substituted 1,3-dienes were then calculated to study the effects of ligands and substrates on regioselectivity. The whole energy profiles for 2-substituted 1,3-diene **1a** with $PCy_3$ as ligand are shown in Fig. 1. Fig. 2 shows the optimized structures of the key stationary points labeled in Fig. 1. The catalyst first undergoes ligand exchange with substrate **1a** to release one $PCy_3$ ligand and afford intermediate **I-1A** (black line in Fig. 1). This process is endergonic by 6.8 kcal/mol. From **I-1A**, 1,2-borocupration (**I-TS1A**) requires an energy barrier of 6.6 kcal/mol relative to the zero point. The oxidative cyclization involving 4,3-borocupration was also calculated (red line in Fig. 1), but the free energy of corresponding transition state **I-TS1B** was found to be 4.5 kcal/mol higher than that of **I-TS1A**. As 4,3-borocupration is irreversible, this constitutes the regioselectivity-determining step of the reaction.

Allyl copper species **I-2A** undergoes ligand exchange via four-membered-ring transition state **I-TS2A**, with a small barrier of 6.1 kcal/mol, to give more-stable 1,4-borocuprated complex **I-3A**. Subsequently, **I-4A** is formed by coordination of *N*-cyanosulfonamide **2a**, and electrophilic cyanation occurs via transition state **I-TS3A**. The calculations showed that electrophilic cyanation is exergonic, and that resulting intermediate **I-5A** is 15.4 kcal/mol lower in energy than **I-4A**. Finally, C−N bond cleavage occurs via transition state **I-TS4A** to give 1,2-borocyanation product **3a** with amine liberation, which has an activation energy barrier of 10.7 kcal/mol relative to **I-5A**. Therefore, the calculations were in agreement with the experimental regioselectivity for 1,2-borocupration over 4,3-borocupration [13].

The calculated free-energy profile for borocyanation of 2-substituted 1,3-diene **1a** with bidentate phosphine XantPhos as ligand is shown in Fig. 3. First, we evaluated the two borocupration modes. The free energy of transition state **I-TS1D** (−6.2 kcal/mol) for 1,2-borocupration was higher than that of **I-TS1C** (−8.5 kcal/mol) for 4,3-borocupration, resulting in a regioselectivity switch from 1,2-borocupration to 4,3-borocupration. **I**−**1C** then undergoes ligand exchange by spanning a barrier of 17.6 kcal/mol (**I-TS2C**) relative to **I**−**1C**, which generates 4,1-borocupration complex **I**−**2C**. Subsequent coordination of **2a** with the Cu center leads to the formation of Cu−cyanide complex **I**−**3C**. Finally, amine is liberated from cyanide via transition state **I-TS4C**, with an energy barrier of 5.8 kcal/mol, to give 4,3-borocyanation product **4a**.

To probe the origins of the regioselectivity for 2-substituted 1,3-diene **1a**, we analyzed the frontier molecular orbitals for both the borylcopper catalyst and substrate **1a**. Fig. 4 shows spatial plots and orbital energies of the relevant frontier molecular orbitals. The energy gap between the LUMO of **1a** and HOMO of the catalyst was much smaller than that between the LUMO of the catalyst and HOMO of **1a**, suggesting that substrate **1a** received electrons and acted as an electrophile in the reactions. The HOMO of the borylcopper catalyst was the Cu−B σ molecular orbital, while the LUMO of **1a** was the $\pi^*$ molecular orbital [27]. Therefore, the LUMO of **1a** played a key role in the regioselectivity. For **1a**, there were two electrophilic sites, namely, the terminal C1 and C4 atoms. As shown in Fig. 4, orbital population analysis found that the 2p orbital of the C1 atom (31.4) made a significantly larger contribution than that of the C4 atom (13.7). Therefore, it is reasonable that borocupration takes place at the C1=C2 bond when $PCy_3$ is used as ligand. When bidentate phosphine ligand XantPhos is used, the dissociation of XantPhos to the monodentate coordination mode is highly endergonic, which accordingly increases the energy barrier of the borocupration step [28]. Therefore, the borocupration steps occurred with the XantPhos ligand in bidentate coordination mode. Transition state **I-TS1D** in the 1,2-borocupration using the bidentate XantPhos ligand experienced greater steric repulsion than **I-TS1C** in the 4,3-borocupration. The optimized geometries indeed show that in **1-TS1d**, the nonbonded distances (C4−H2 and C5−H1) between the phenyl group of **1a** and the phenyl group of XantPhos are shorter than the sum of the van der Waals radii of the relevant elements (2.90 Å for C−H) [29]. However, no such steric repulsion

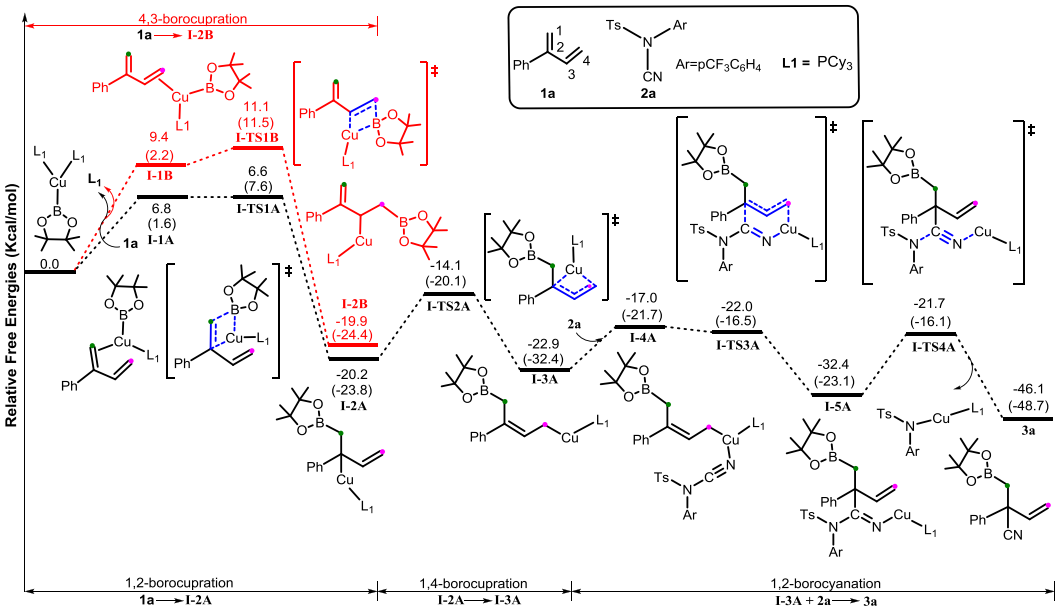


**Fig. 1.** Calculated energy profiles for Cu-catalyzed borylation reaction of 2-substituted 1,3-diene **1a** with $PCy_3$ as ligand (black and red lines indicate 1,2-borocupration and 4,3-borocupration, respectively). Values shown are relative free energies calculated by M06/BS2 and B3LYP/BS1 (in parentheses) in kcal/mol. (For interpretation of the references to colour in this figure legend, the reader is referred to the Web version of this article.)

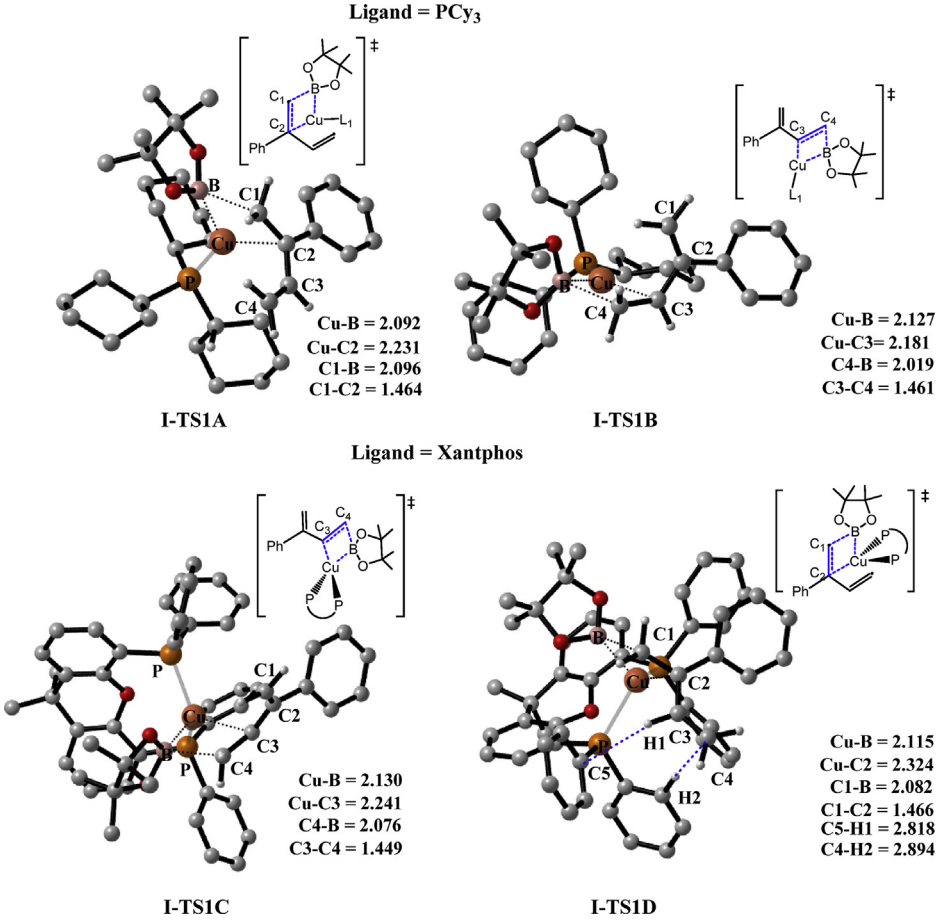


**Fig. 2.** Optimized structures of key species labeled in Figs. 1 and 3. Key bond lengths are given in Å; trivial H atoms are omitted for clarity.

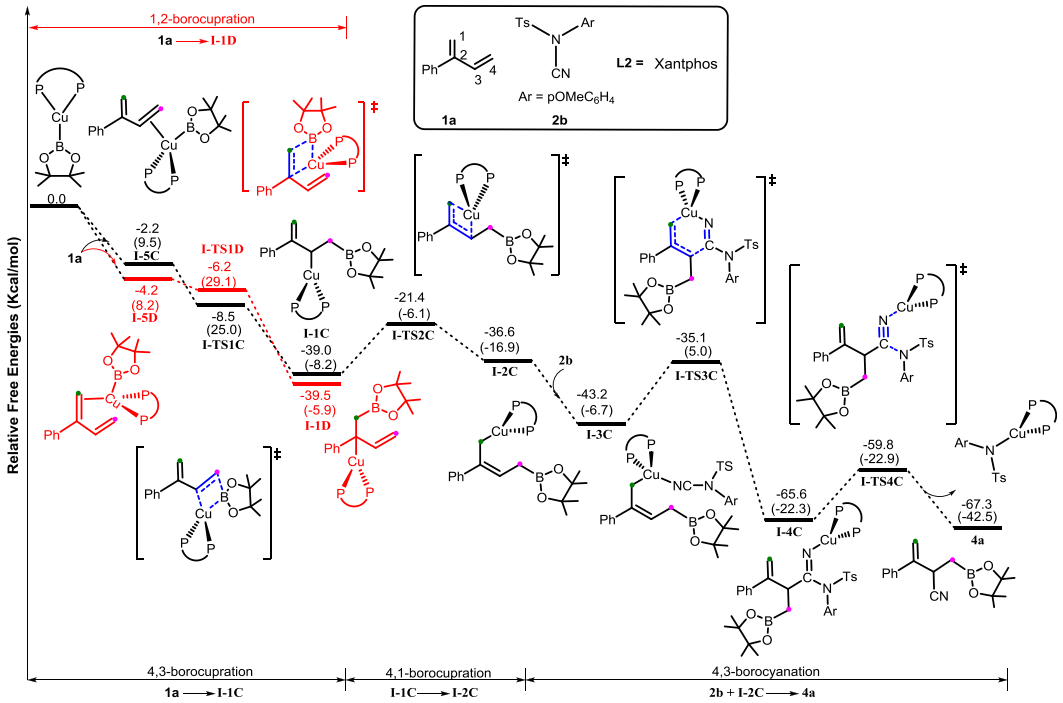


**Fig. 3.** Calculated energy profiles for Cu-catalyzed borylation reaction of 2-substituted 1,3-diene **1a** with XantPhos as ligand (black and red lines indicate 4,3-borocyanation and 1,2-borocyanation, respectively). Values shown are relative free energies calculated by M06/BS2 and B3LYP/BS1 (in parentheses) in kcal/mol. (For interpretation of the references to colour in this figure legend, the reader is referred to the Web version of this article.)

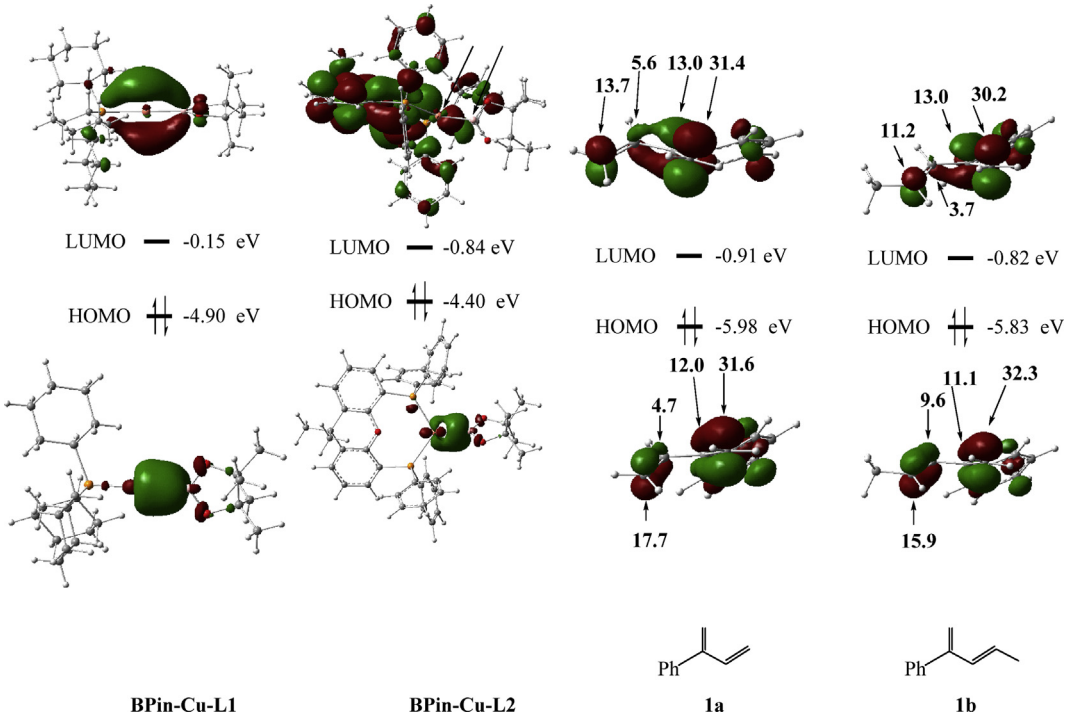


**Fig. 4.** Frontier molecular orbitals calculated for the borylcopper catalyst, and 2-substituted (**1a**) and 2,4-disubstituted (**1b**) 1,3-dienes. Orbital energies are given in eV.

exists in **1-TS1c**, which thus results in **1-TS1c** being more favored than **1-TS1d**. This result can be further supported by the RDG analysis (Scheme S5). Therefore, steric factors were dominant in determining the regioselectivity of the reaction using the bidentate XantPhos ligand.

To further verify that steric factors were dominant in determining the regioselectivity of the reaction using the bidentate XantPhos ligand, we replaced the hydrogen atom at C4 in **1a** with a methyl group and computed the 4,3- and 1,2-borocupration steps. For 2,4-disubstitued 1,3-diene **1b**, the bulky methyl group still effectively promoted 1,2-borocupration, and induced the barrier difference (4.6 kcal/mol) between 4,3- and 1,2-borocupration for

the reaction using $PCy_3$ as ligand (Fig. 5a). For the reaction using the bidentate XantPhos ligand (Figs. 5b), 1,2-borocupration (**II-TS1C**, −5.1 kcal/mol) was able to override 4,3-borocupration (**II-TS1D**, −3.9 kcal/mol) of **1b**. Therefore, both electronic and steric effects favored 1,2-borocupration for 2,4-disubstitued 1,3-dienes, regardless of the ligand used.

We attempted to computationally expand the ligand scope for 2-substituted 1,3-diene **1a** to further verify the factors that determine regioselectivity. The energy profiles in the presence of monodentate Sphos and bidentate dppe ligands (Fig. 6), which have been used in the borocupration of 1-substituted 1,3-diene **1c** [14], were examined. For the monodentate Sphos ligand (Fig. 6a), the barrier for the 4,3-borocupration step (4.3 kcal/mol) was higher than that for the 1,2-borocupration step (1.1 kcal/mol). In contrast, for bidentate ligand dppe, the free energy of transition state **I-TS1H** (5.4 kcal/mol) for 1,2-borocupration is higher than that of **I-TS1G** (−0.3 kcal/mol) for 4,3-borocupration, meaning that the regioselectivity could still be switched (Fig. 6b). Therefore, a bidentate ligand, such as XantPhos or dppe, does not provide the convenience of ligand dissociation, resulting in instability in the transition state for 1,2-borocupration of **1a**. When monodentate ligands $PCy_3$ and Sphos were used in the calculations, 1,2-borocupration was preferred over 4,3-borocupration for **1a**.

We further elucidated the origin of substrate-controlled regioselectivity by investigating the Cu-catalyzed borylation reaction in the presence of 1-substituted, 1,2-disubstituted, and 1,3-disubstituted 1,3-dienes, which were used in experiments reported by Meng and coworkers [14]. The calculated overall energy profile is shown in Fig. 7. In agreement with experimental observations, the calculations indicated that 1,2-borocupration was less favorable than 4,3-borocupration for the three substrates, regardless of the ligand ($PCy_3$ or XantPhos). These results were consistent with the relative orbital percentage contribution of the two carbon atoms, C1 and C4, in the LUMO of the three substrates (Fig. 8).

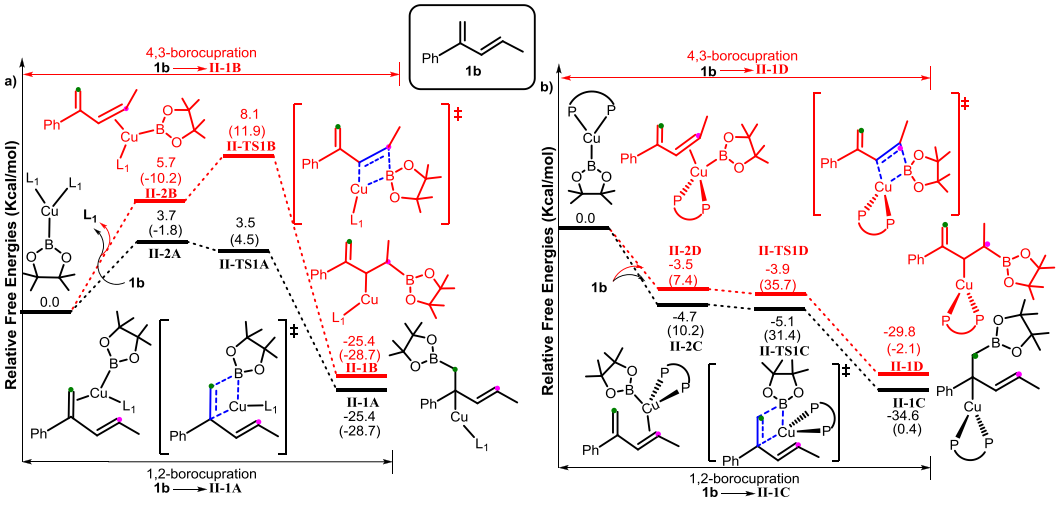


**Fig. 5.** Calculated energy profiles for regioselectivity-determining steps of 2,4-disubstituted 1,3-diene **1b** with XantPhos and $PCy_3$ ligands. Values shown are relative free energies calculated by M06/BS2 and B3LYP/BS1 (in parentheses) in kcal/mol.

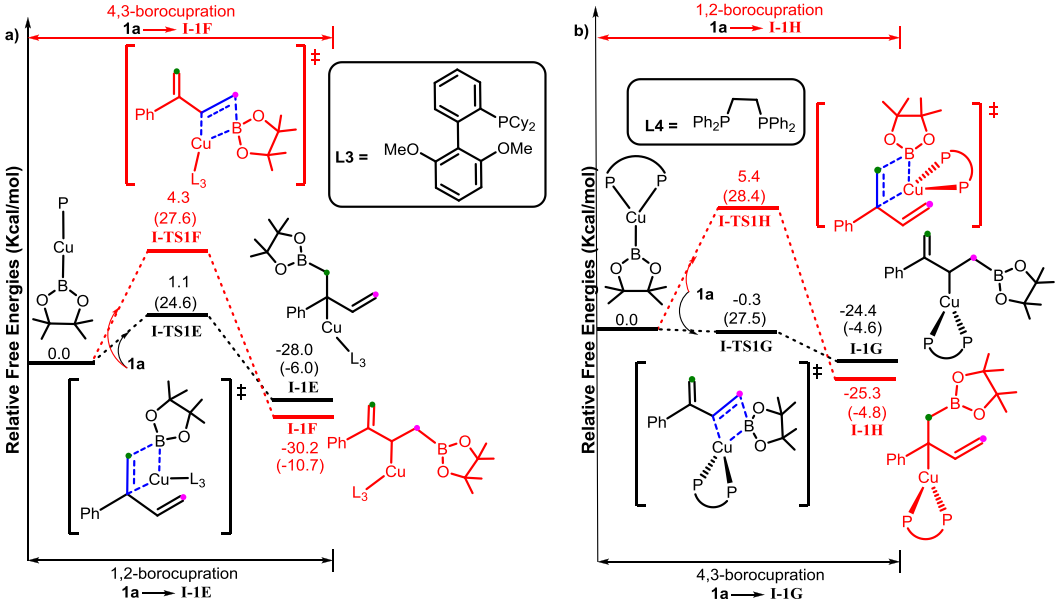


**Fig. 6.** Calculated energy profiles for regioselectivity-determining steps with Sphos and dppe ligands for 2-substituted 1,3-diene **1a**. Values shown are relative free energies calculated by M06/BS2 and B3LYP/BS1 (in parentheses) in kcal/mol.

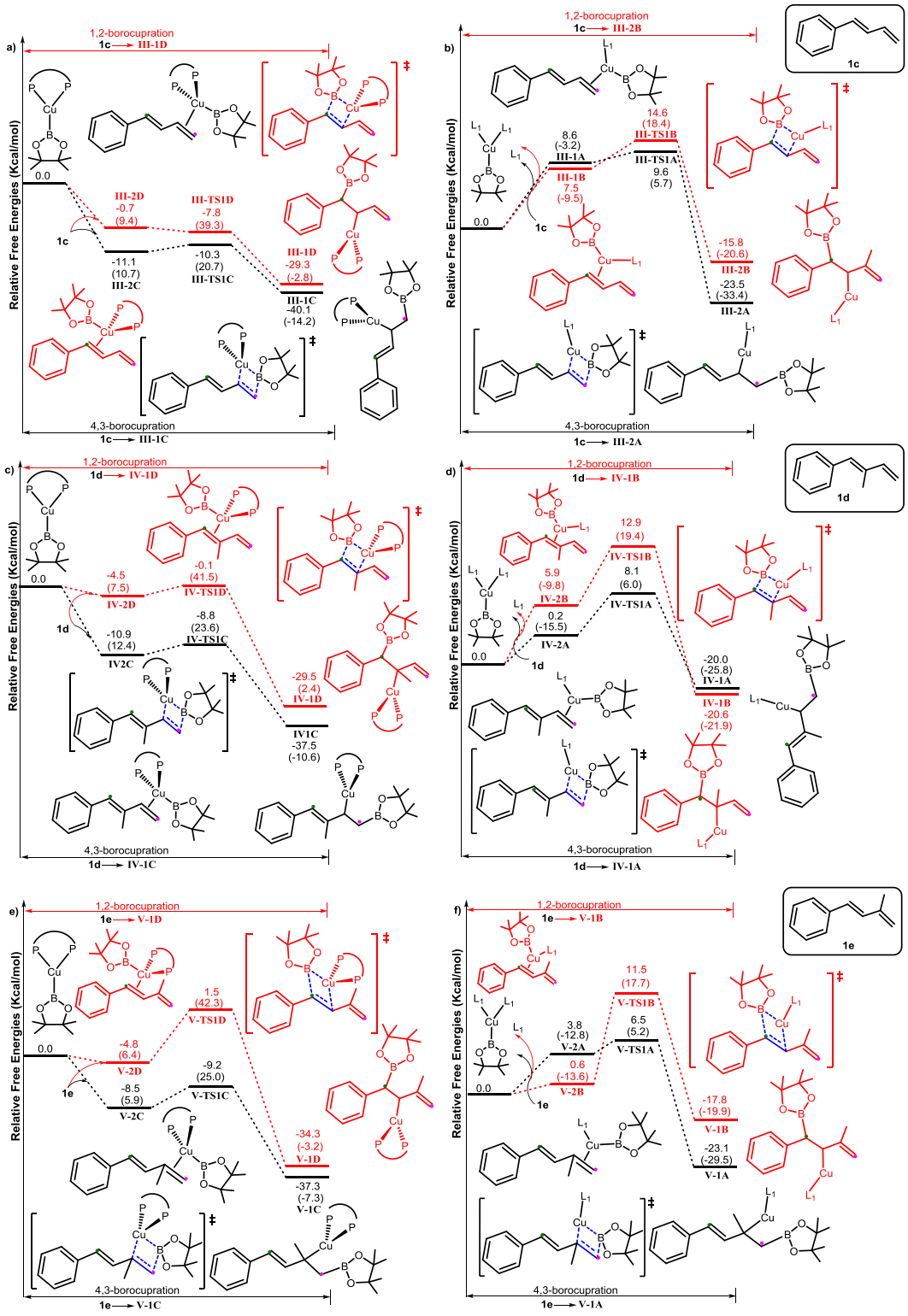


**Fig. 7.** Calculated energy profiles for regioselectivity-determining steps with $PCy_3$ and XantPhos ligands for 1-substituted (**1c**), 1,2-disubstituted (**1d**), and 1,3-disubstituted (**1e**) 1,3-dienes. Values shown are relative free energies calculated by M06/BS2 and B3LYP/BS1 (in parentheses) in kcal/mol.

Furthermore, the steric effects also favored 4,3-borocupration.

## 4. Conclusions

The regioselectivity of the Cu-catalyzed borylcyanation of non-symmetrically substituted 1,3-dienes was theoretically studied using DFT calculations at the B3LYP level. The computational results showed that monodentate ligands $PCy_3$ and SPhos can favor 1,2-borocupration over 4,3-borocupration in 2-substituted 1,3-dienes. However, 4,3-borocupration is facilitated and 1,2-borocupration can be avoided when large bidentate ligands, such as XantPhos and dppe, are present. The 1-substituted, 1,2-disubstituted, and 1,3-

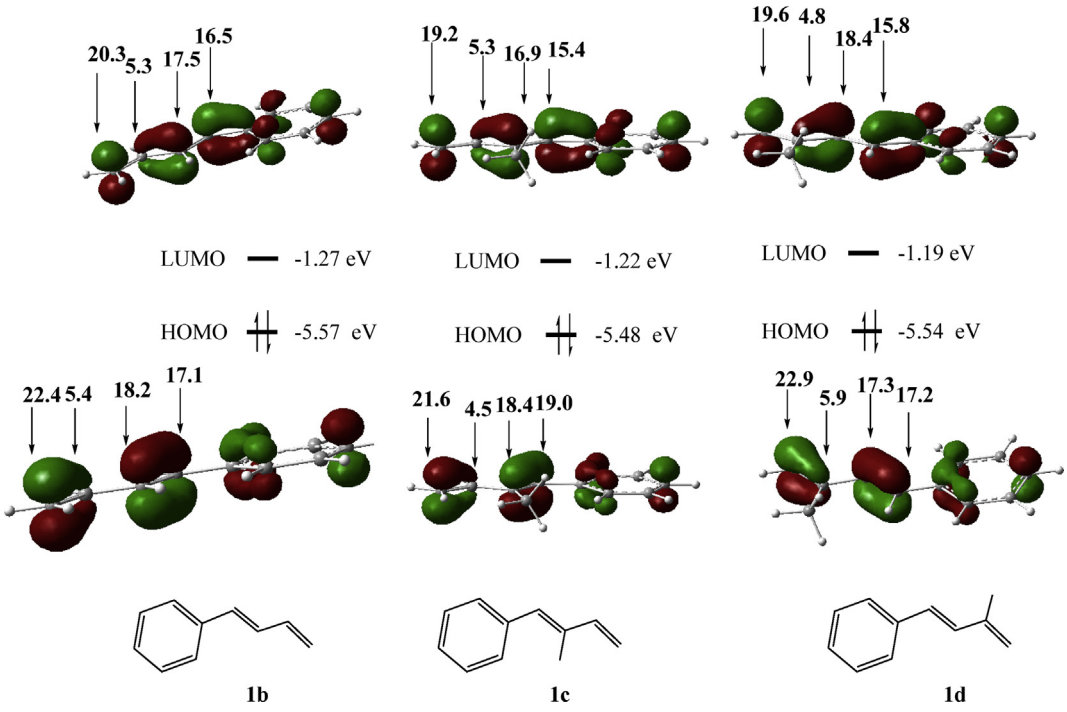


**Fig. 8.** Frontier molecular orbitals calculated for 1-substituted (**1c**), 1,2-disubstituted (**1d**), and 1,3-disubstituted (**1e**) 1,3-dienes. Orbital energies are given in eV.

disubstituted 1,3-dienes enabled 4,3-borocupration, while 2,4-disubstituted 1,3-dienes favored 1,2-borocupration, irrespective of the presence of bidentate or monodentate ligands. Analysis of the frontier molecular orbitals suggested that the borylcyanation step was a nucleophilic attack of the Cu–B σ bond at the coordinated 1,3-diene. The different regioselectivities for different substrates and ligands can be attributed to different electronic and steric factors. These theoretical results will aid understanding of other borocupration reactions in a wide range of substrates and could be used for ligand design. We believe these theoretical results are inspiring for future ligand design of other borocupration reactions.

## Declaration of competing interest

The authors declare that they have no known competing financial interests or personal relationships that could have appeared to influence the work reported in this paper.

## Acknowledgements

This work was supported by the National Natural Science Foundation of China (Grant No. 21573095), the Science and Technology Program of Guangzhou (Grant No. 201707010269), and the high-performance computing platform of Jinan University.

## Appendix A. Supplementary data

Supplementary data to this article can be found online at https://doi.org/10.1016/j.jorganchem.2019.121014.

## References

[1] (For selected reviews, see) (a) A. Minatti, K. MuÇiz, Chem. Soc. Rev. 36 (2007) 1142–1152;
(b) J.R. Wolstenhulme, V. Gouverneur, Acc. Chem. Res. 47 (2014) 3560–3570;
(c) M.S. Sigman, E.W. Werner, Acc. Chem. Res. 45 (2012) 874–884;
(d) D. Wang, A.B. Weinstein, P.B. White, S.S. Stahl, Chem. Rev. 118 (2018) 2636–2679.
[2] (For recent reviews, see) (a) D.S. Muller, I. Marek, Chem. Soc. Rev. 45 (2016) 4552–4566;
(b) X. Zhu, S. Chiba, Chem. Soc. Rev. 45 (2016) 4504–4523;
(c) M. Shibasaki, M. Kanai, Chem. Rev. 108 (2008) 2853–2873;
(d) S. Thapa, B. Shrestha, S.K. Gurung, R. Giri, Org. Biomol. Chem. 13 (2015) 4816–4827;
(e) C. Maaliki, E. Thiery, J. Thibonnet, Eur. J. Org. Chem. (2017) 209–228;
(f) N. Yoshikai, E. Nakamura, Chem. Rev. 112 (2012) 2339–2372.
[3] (For selected examples, see) (a) W. Su, T.-J. Gong, X. Lu, M.-Y. Xu, C.-G. Yu, Z.-Y. Xu, H.-Z. Yu, B. Xiao, Y. Fu, Angew. Chem. Int. Ed. 54 (2015) 12957–12961;
(b) R. Sakae, K. Hirano, M. Miura, J. Am. Chem. Soc. 137 (2015) 6460–6463;
(c) Y. Huang, K.B. Smith, M.K. Brown, Angew. Chem. Int. Ed. 56 (2017) 13314–13318;
(d) B. Chen, P. Cao, Y. Liao, M. Wang, J. Liao, Org. Lett. 20 (2018) 1346–1349;
(e) K.M. Logan, M.K. Brown, Angew. Chem. Int. Ed. 56 (2017) 851–855;
(f) T. Itoh, Y. Kanzaki, Y. Shimizu, M. Kanai, Angew. Chem. Int. Ed. 57 (2018) 8265–8401;
(g) G. Zhang, A. Cang, Y. Wang, Y. Li, G. Xu, Q. Zhang, T. Xiong, Q. Zhang, Org. Lett. 20 (2018) 1798–1801;
(h) H.-M. Wang, H. Zhou, Q.-S. Xu, T.-S. Liu, C.-L. Zhuang, M.-H. Shen, H.-D. Xu, Org. Lett. 20 (2018) 1777–1780;
(i) F. Cheng, W. Lu, W. Huang, L. Wen, M. Li, F. Meng, Chem. Sci. 9 (2018) 4992–4998;
(j) B. Chen, P. Cao, X. Yin, Y. Liao, L. Jiang, J. Ye, M. Wang, J. Liao, ACS Catal. 7 (2017) 2425–2429;
(k) K. Semba, Y. Ohtagaki, Y. Nakao, Org. Lett. 18 (2016) 3956–3959;
(l) A.R. Burns, J.S. Gonzalez, H.W. Lam, Angew. Chem. Int. Ed. 51 (2012) 10827–10831;
(m) J.J. Smith, D. Best, H.W. Lam, Chem. Commun. 52 (2016) 3770–3772;
(n) T. Jia, P. Cao, B. Wang, Y. Lou, X. Yin, M. Wang, J. Liao, J. Am. Chem. Soc. 137 (2015) 13760–13763;
(o) J. Lee, S. Radomkit, S. Torker, J. del Pozo, A.H. Hoveyda, Nat. Chem. 10 (2017) 99–108;
(p) N. Kim, J.T. Han, D.H. Ryu, J. Yun, Org. Lett. 19 (2017) 6144–6147.
[4] (For selected examples, see) (a) Y. Sadaki, C. Zhong, M. Sawamura, H. Ito, J. Am. Chem. Soc. 132 (2010) 1226–1227;
(b) L. Jiang, P. Cao, M. Wang, B. Chen, B. Wang, J. Liao, Angew. Chem. Int. Ed. 55 (2016) 13854–13858;
(c) X. Li, F. Meng, S. Torker, Y. Shi, A.H. Hoveyda, Angew. Chem. Int. Ed. 55 (2016) 9997–10002;
(d) K.B. Smith, M.K. Brown, J. Am. Chem. Soc. 139 (2017) 7721–7724;
(e) S.R. Sardini, M.K. Brown, J. Am. Chem. Soc. 139 (2017) 9823–9826;
(f) K.B. Smith, Y. Huang, M.K. Brown, Angew. Chem. Int. Ed. 57 (2018) 6146–6149;
(g) T. Iwasaki, R. Shimizu, R. Imanishi, H. Kuniyasu, N. Kambe, Angew. Chem. Int. Ed. 54 (2015) 9347–9350;

(h) Y.-Y. Gui, N. Hu, X.-W. Chen, L.-L. Liao, T. Ju, J.-H. Ye, Z. Zhang, J. Li, D.-G. Yu, J. Am. Chem. Soc. 139 (2017) 17011–17014;
(i) H.E. Burks, L.T. Kliman, J.P. Morken, J. Am. Chem. Soc. 131 (2009) 9134–9135;
(j) R.J. Ely, J.P. Morken, J. Am. Chem. Soc. 132 (2010) 2534–2535.

[5] (For selected examples, see) (a) F. Meng, H. Jang, B. Jung, A.H. Hoveyda, Angew. Chem. Int. Ed. 52 (2013) 5046–5051;
(b) F. Meng, K.P. McGrath, A.H. Hoveyda, Nature 513 (2014) 367–374;
(c) H. Jang, F. Romiti, S. Torker, A.H. Hoveyda, Nat. Chem. 9 (2017) 1269–1275;
(d) A. Boreux, K. Indukuri, F. Gagosz, O. Riant, ACS Catal. 7 (2017) 8200–8204;
(e) K. Yeung, R.E. Ruscoe, J. Rae, A.P. Pulis, D.J. Procter, Angew. Chem. Int. Ed. 55 (2016) 11912–11916;
(f) F. Meng, X. Li, S. Torker, Y. Shi, X. Shen, A.H. Hoveyda, Nature 537 (2016) 387–393. Angew. Chem. 128 (2016) 12091;
(g) A. Sawada, T. Fujihara, Y. Tsuji, Adv. Synth. Catal. 360 (2018) 2621.

[6] (For selected examples, see) (a) W. Su, T.-J. Gong, Q. Zhang, B. Xiao, Y. Fu, ACS Catal. 6 (2016) 6417–6421;
(b) L. Mao, R. Bertermann, K. Emmert, K.J. Szabo, T.B. Marder, Org. Lett. 19 (2017) 6586–6589;
(c) M. Xiong, X. Xie, Y. Liu, Org. Lett. 19 (2017) 3398–3401;
(d) P. Liu, Y. Fukui, P. Tian, Z.T. He, C.Y. Sun, N.Y. Wu, G.Q. Lin, J. Am. Chem. Soc. 135 (2013) 11700–11703.

[7] (For selected examples, see:) (a) Y. Sasaki, Y. Horita, C. Zhong, M. Sawamura, H. Ito, Angew. Chem. Int. Ed. 50 (2011) 2778–2782;
(b) F. Meng, F. Haeffner, A.H. Hoveyda, J. Am. Chem. Soc. 136 (2014) 11304–11307;
(c) X.F. Wei, X.W. Xie, Y. Shimizu, M. Kanai, J. Am. Chem. Soc. 139 (2017) 4647–4650.

[8] D. Li, Y.E. Kim, J. Yun, Org. Lett. 17 (2015) 860–863.

[9] (For selected examples, see) (a) Y. Shimizu, M. Kanai, Tetrahedron Lett. 55 (2014) 3727–3737;
(b) K. Semba, T. Fujihara, J. Terao, Y. Tsuji, Tetrahedron 71 (2015) 2183–2197;
(c) H. Yoshida, ACS Catal. 6 (2016) 1799–1811.

[10] (a) A.J. Fatiadi, in: S. Patai, Z. Rappaport (Eds.), In Preparation and Synthetic Applications of Cyano Compounds, Wiley, 1983;
(b) F.F. Fleming, Nat. Prod. Rep. 16 (1999) 597–606;
(c) J.S. Miller, J.L. Manson, Acc. Chem. Res. 34 (2001) 563–570;
(d) F.F. Fleming, L. Yao, P.C. Ravikumar, L. Funk, B.C. Shook, J. Med. Chem. 53 (2010) 7902–7917.

[11] (For the synthesis of NCTS, see) (a) F. Kurzer, J. Chem. Soc. (1949) 1034–1038;
(b) F. Kurzer, J. Chem. Soc. (1949) 3029–3033 (For pioneering work on the application of NCTS in transition metal catalysis, see);
(c) P. Anbarasan, H. Neumann, M. Beller, Angew. Chem. Int. Ed. 50 (2011) 519–522.

[12] (a) Y. Yang, S.L. Buchwald, Angew. Chem. Int. Ed. 53 (2014) 8677–8681;
(b) Y. Yang, P. Liu, ACS Catal. 5 (2015) 2944–2951;
(c) Y. Yang, Angew. Chem. Int. Ed. 55 (2016) 345–349;
(d) W. Zhao, J. Montgomery, Angew. Chem. Int. Ed. 54 (2015) 12683–12686;
(e) W. Zhao, J. Montgomery, J. Am. Chem. Soc. 138 (2016) 9763–9766;
(f) S.J. He, B. Wang, X. Lu, T.J. Gong, Y.N. Yang, X.X. Wang, Y. Wang, B. Xiao, Y. Fu, Org. Lett. 20 (2018) 5208–5212.

[13] (a) T. Jia, Q. He, R.E. Ruscoe, A.P. Pulis, D.J. Procter, Angew. Chem. Int. Ed. 57 (2018) 11305–11309;
(b) T. Jia, M.J. Smith, A.P. Pulis, G.J.P. Perry, D.J. Procter, ACS Catal. 9 (2019) 6744–6750.

[14] L. Wen, H. Zhang, J. Wang, F. Meng, Chem. Commun. 54 (2018) 12832–12835.

[15] (a) A.D. Becke, Density-functional thermochemistry. III. The role of exact exchange, J. Chem. Phys. 98 (1993) 5648–5652;
(b) C. Lee, W. Yang, R.G. Parr, Development of the colie-salvetti correlation-energy formula into a functional of the electron density, Phys. Rev. B. 37 (1988) 785–789;
(c) P.J. Stephens, F.J. Devlin, C.F. Chabalowski, M.J. Frisch, Ab initio calculation of vibrational absorption and circular dichroism spectra using density functional force fields, J. Phys. Chem. 98 (1994) 11623–11627.

[16] A.V. Marenich, C.J. Cramer, D.G.J. Truhlar, Phys. Chem. B 113 (2009) 4538–4543.

[17] M.J. Frisch, G.W. Trucks, H.B. Schlegel, G.E. Scuseria, M.A. Robb, J.R. Cheeseman, G. Scalmani, V. Barone, B. Mennucci, G.A. Petersson, H. Nakatsuji, M. Caricato, X. Li, H.P. Hratchian, A.F. Izmaylov, J. Bloino, G. Zheng, J.L. Sonnenberg, M. Hada, M. Ehara, K. Toyota, R. Fukuda, J. Hasegawa, M. Ishida, T. Nakajima, Y. Honda, O. Kitao, H. Nakai, T. Vreven, J.A. Montgomery Jr., J.E. Peralta, F. Ogliaro, M. Bearpark, J.J. Heyd, E. Brothers, K.N. Kudin, V.N. Staroverov, T. Keith, R. Kobayashi, J. Normand, K. Raghavachari, A. Rendell, J.C. Burant, S.S. Iyengar, J. Tomasi, M. Cossi, N. Rega, J.M. Millam, M. Klene, J.E. Knox, J.B. Cross, V. Bakken, C. Adamo, J. Jaramillo, R. Gomperts, R.E. Stratmann, O. Yazyev, A.J. Austin, R. Cammi, C. Pomelli, J.W. Ochterski, R.L. Martin, K. Morokuma, V.G. Zakrzewski, G.A. Voth, P. Salvador, J.J. Dannenberg, S. Dapprich, A.D. Daniels, O. Farkas, J.B. Foresman, J.V. Ortiz, J. Cioslowski, D.J. Fox, Gaussian 09, Revision E.01, Gaussian, Inc., Wallingford CT, 2013.

[18] (a) K. Fukui, J. Phys. Chem. 74 (1970) 4161–4163;
(b) K. Fukui, Acc. Chem. Res. 14 (1981) 363–368.

[19] (a) P.J. Hay, W.R. Wadt, J. Chem. Phys. 82 (1985) 299;
(b) W.R. Wadt, P.J. Hay, J. Chem. Phys. 82 (1985) 284.

[20] A.W. Ehlers, M. Böhme, S. Dapprich, A. Gobbi, A. Höllwarth, V. Jonas, K.F. Köhler, R. Stegmann, A. Veldkamp, G. Frenking, Chem. Phys. Lett. 208 (1993) 111–114.

[21] (a) R. Krishnan, J.S. Binkley, R. Seeger, J.A. Pople, J. Chem. Phys. 72 (1980) 650;
(b) A.D. McLean, G.S. Chandler, J. Chem. Phys. 72 (1980) 5639.

[22] (a) Y. Zhao, N.E. Schultz, D.G. Truhlar, Exchange-correlation functional with broad accuracy for metallic and nonmetallic compounds, kinetics, and noncovalent interactions, J. Chem. Phys. 123 (2005), 161103/1–161103/4;
(b) Y. Zhao, D.G. Truhlar, Density functionals with broad applicability in chemistry, Acc. Chem. Res. 41 (2008) 157–167;
(c) Y. Zhao, D.G. Truhlar, The M06 suite of density functionals for main group thermochemistry, thermochemical kinetics, noncovalent interactions, excited states, and transition elements: two new functionals and systematic testing of four M06-class functionals and 12 other functionals, Theor. Chem. Acc. 120 (2008) 215–241;
(d) Y. Zhao, D.G. Truhlar, Benchmark energetic data in a model system for grubbs II metathesis catalysis and their use for the development, assessment, and validation of electronic structure methods, J. Chem. Theory Comput. 5 (2009) 324–333.

[23] F. Weigend, R. Phys Ahlrichs, Chem. Chem. Phys. 7 (2005) 3297–3305.

[24] S. Grimme, J. Antony, S. Ehrlich, H. Krieg, J. Chem. Phys. 132 (2010) 154104.

[25] T. Lu, F.W. Chen, J. Comput. Chem. 33 (2012) 580–592.

[26] During the submission of this manuscript, a related DFT calculations on borylcyanation of 1,3-diene was published, see: X. Li, H. Wu, Z. Wu, G. Huang J. Org. Chem. 84 (2019) 5514–5523.

[27] (For similar explanation, see) (a) L. Dang, Z.Y. Lin, T.B. Marder, Organometallics 27 (2008) 4443–4454;
(b) L. Dang, H.T. Zhao, Z.Y. Lin, T.B. Marder, Organometallics 26 (2007) 2824–2832;
(c) L. Dang, Z.Y. Lin, T.B. Marder, Chem. Commun. (2009) 3987–3995.

[28] For similar explanation, see Q. Lu, B. Wang, H. Yu, Y. Fu, ACS Catal. 5 (2015) 2062–2069.

[29] R.S. Rowland, R. Taylor, J. Phys. Chem. 100 (1996) 7384.